Visual Neuroscience (1995), **12**, 545–561. Printed in the USA.

Simulation of an anatomically defined local circuit: The cone-horizontal cell network in cat retina

ROBERT G. SMITH
Department of Neuroscience, University of Pennsylvania, Philadelphia

(RECEIVED July 22, 1994; ACCEPTED November 28, 1994)

Abstract

The outer plexiform layer of the retina contains a neural circuit in which cone synaptic terminals are electrically coupled and release glutamate onto wide-field and narrow-field horizontal cells. These are also electrically coupled and feed back through a GABAergic synapse to cones. In cat this circuit's structure is known in some detail, and much of the chemical architecture and neural responses are also known, yet there has been no attempt to synthesize this knowledge. We constructed a large-scale compartmental model (up to 50,000 compartments) to incorporate the known anatomical and biophysical facts. The goal was to discover how the various circuit components interact to form the cone receptive field, and thereby what possible function is implied. The simulation reproduced many features known from intracellular recordings: (1) linear response of cone and horizontal cell to intensity, (2) some aspects of temporal responses of cone and horizontal cell, (3) broad receptive field of the wide-field horizontal cell, and (4) center-surround cone receptive field (derived from a "deconvolution model"). With the network calibrated in this manner, we determined which of its features are necessary to give the cone receptive field a Gaussian center-surround shape. A Gaussian-like center that matches the center derived from the ganglion cell requires both optical blur and cone coupling: blur alone is too narrow, coupling alone gives an exponential shape without a central dome-shaped peak. A Gaussian-like surround requires both types of horizontal cell: the narrow-field type for the deep, proximal region and the wide-field type for the shallow, distal region. These results suggest that the function of the cone-horizontal cell circuit is to reduce the influence of noise by spatio-temporally filtering the cone signal before it passes through the first chemical synapse on the pathway to the brain.

Keywords: Retina, Receptive field, Feedback, Computer simulation, Compartmental model

Introduction

As a visual signal travels from a cone outer segment to the brain, it passes through a complex circuit intrinsic to the outer retina. The hub of this circuit is the cone axon terminal ("pedicle"), and its basic plan is strikingly similar across vertebrate species (Lasansky, 1971, 1973; Kolb, 1970, 1977). After traversing this neural circuit, the visual signal is transmitted through a chemical synapse, which, due to biological constraints, limits the signal's range by adding distortion and noise (Laughlin et al., 1987). It has been postulated that the cone pedicle circuit filters the signal to reduce its dynamic range, lessening the effect of these limitations (Attwell, 1986). Since the filter provides input to the rest of the visual system, how and why it transforms signals is of considerable interest.

In mammals and some other vertebrates the cone pedicle forms electrical synapses with its neighbors (Kolb, 1977; Raviola & Gilula, 1975, Smith et al., 1986), and chemical synapses with generally two types of horizontal cell, known in cat and rabbit as HA and HB (Fig. 1; Fisher & Boycott, 1974; Kolb, 1974; Boycott et al., 1978; but see Peichl & Gonzalez-Soriano, 1994). HA and HB cells differ by a factor of 2 in dendritic-field width and number of cone contacts (Wässle et al., 1978*a*). Both are coupled electrically to neighbors of their own type, though to different extents (Kolb, 1977; Vaney, 1991, 1993), and both types are GABAergic (Chun & Wässle, 1989; Sarthy & Fu, 1989; Vardi et al., 1994).

In salamander, fish, and turtle the evidence for negative feedback onto the pedicle is direct, from intracellular recordings (Attwell et al., 1983; Baylor et al., 1971; Tachibana & Kaneko, 1984; Murakami et al., 1982; Piccolino et al., 1981; Skrzypek & Werblin, 1983; Werblin, 1974; Wu, 1991; but see Lasansky, 1981; Burkhardt, 1993). The feedback is mediated through chloride (Tachibana & Kaneko, 1984; Attwell et al., 1987; Wu, 1991). In mammals, the evidence is indirect and includes the demonstrations that depolarizing a horizontal cell antagonizes the light response of both on- and off-center ganglion cells (Mangel, 1991) and that oscillations at 40–50 Hz can be elic-

Reprint requests to: Robert G. Smith, University of Pennsylvania, Rm 123, Anat-Chem Bldg., 37th and Service Dr., Philadelphia, PA 19104-6058, USA.

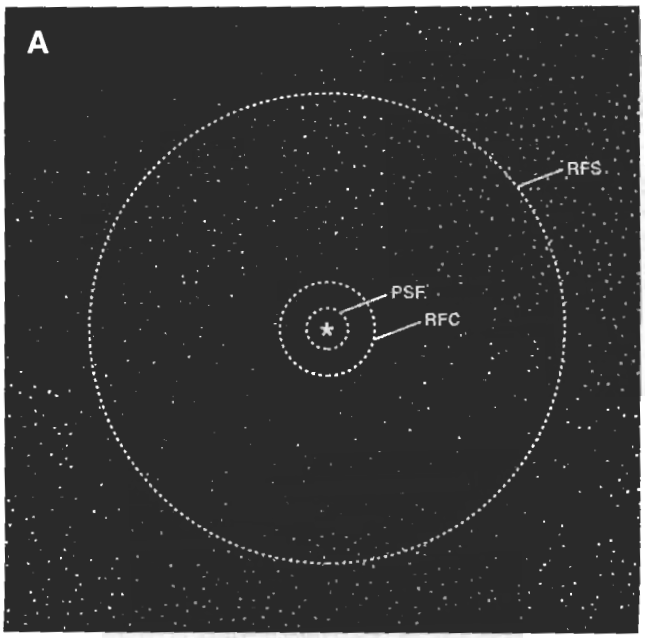

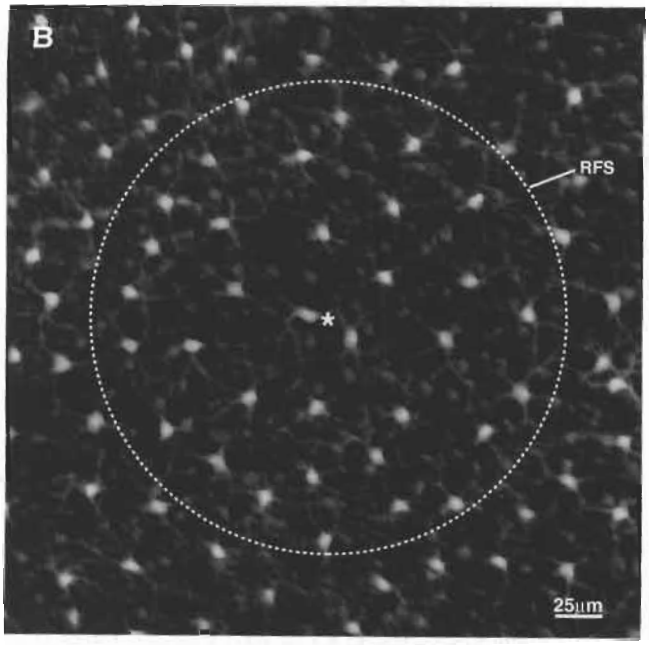

Fig. 1. A: Cone array in cat retina (tangential, 1-μm section stained with toluidine blue) near 1-deg eccentricity, showing regular nature of cone spacing. Density is ~24,000/mm^2. Superimposed circles represent diameter (at 1/e peak) of Gaussian approximations to optical and receptive-field components. Point-spread function of cat's optics (PSF) includes about ten cones, receptive-field center of one cone (RFC) includes about 50 cones, and receptive-field surround (RFS) includes about 1500 cones. B: Tangential view of cat horizontal cell arrays near 1-deg eccentricity stained with antibody to calbindin. Strongly stained cells (lightest appearing) are type A, pale cells are type B. Grayscale of both images is inverted (the black background represents no stain). Tissue prepared by S. Kumar and photographed by P. Auerbach.

ited in the horizontal cell that almost certainly arise from feedback (van de Grind & Grüsser, 1981).

Thus, the circuit looks like a spatial bandpass filter (Fig. 2): cone coupling would remove high spatial frequencies and horizontal cell feedback would remove lower spatial frequencies. An estimate of the cone center-surround profile derived from ganglion cell measurements suggests that the cone surround should be weak (Smith & Sterling, 1990). However, few detailed measurements have been made of the spatiotemporal properties of the cone receptive field in mammals. Records by Nelson (1977) from the cat cone *in situ* suggest, as might be expected from electrical coupling, a rather broad spatial response, consistent with evidence from lower vertebrates (Baylor et al., 1971; Detwiler & Hodgkin, 1979; Kraft & Burkhardt, 1986; Normann et al., 1984; Attwell et al., 1984). The inhibitory cone surround that would be expected from GABAergic feedback, observed in lower vertebrates, was not observed in cat. But the records were not of ideal quality and have never been repeated.

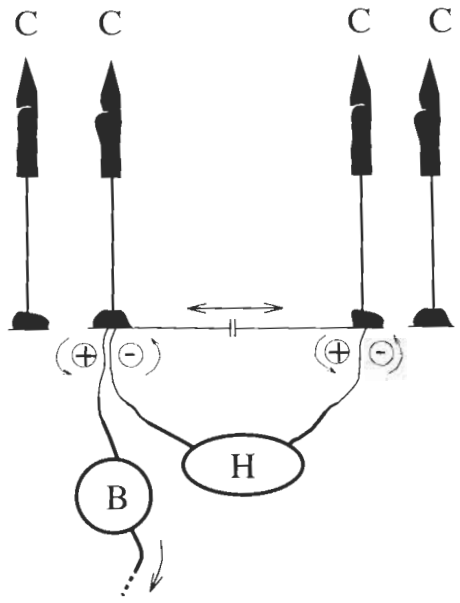

Fig. 2. Simplified schematic of cone-horizontal circuit showing cone-cone coupling by gap junctions (horizontal arrow), feedforward chemical synapse (+) to bipolar and horizontal cells, and feedback (−) from horizontal cells. Horizontal cells are also coupled by gap junctions (not illustrated). C: cone; H: horizontal cell; and B: bipolar cell.

What remains unclear is how the individual components of this circuit interact and why they are necessary. For example, the cone's receptive-field center is probably shaped by optical blur and cone coupling, but what are their respective contributions? Similarly, the cone's receptive-field surround is probably shaped by both wide-field and narrow-field cells, but why the two types? Such questions are not easily addressed by direct experiment. Where recording is easiest (lower vertebrates), neither the natural optics nor the overall structure of the circuit have been quantified. Where the optics and the circuit structure have been quantified (mammals), the physiological descriptions are incomplete. Even if all the information were available for a given species regarding optics, connections, and receptive fields, a dynamic model would be required to establish the key interactions.

We report here a biophysically based computer simulation of the circuit underlying the cone receptive field in the cat *area centralis*. The strategy was to start with an "anatomically correct" model incorporating basic facts such as the known optics, density of the three neuron types, and their synaptic connec-

tions. We modeled each neuron according to published data when available. When data was unavailable, we attempted to select parameter values that were constrained by facts.

The simulation had three objectives: (1) to determine whether constructing an anatomically defined model based on "reasonable" physiological parameters would actually produce realistic resting potentials and receptive fields where this information was known, i.e. in horizontal cells. Such an attempt could fail if it required elements omitted from the model, for example, nonlinear elements such as voltage-sensitive channels. (2) Determine a set of "standard" parameters for which such a model would produce a reasonable center-surround receptive field for the cone. By reasonable is meant a receptive field that would sum over space to form the beta ganglion cell receptive field (Smith & Sterling, 1990; Cohen & Sterling, 1989; Cleland et al., 1979). (3) Under the conditions where the simulation produced a center-surround cone receptive field, determine contributions of the various elements in defining the filter, and study the interactions between them.

Methods

Computation

We simulated the cone-horizontal circuit as a compartmental model defined with the simulation language "NeuronC" (Smith, 1992). The circuit was constructed from "neural elements" (cable, synapse, gap junction, etc.) predefined in the simulation language. A short description (350 lines) defined the anatomical structure of the neural circuit and its synaptic interconnections. From this description, the simulator generated a series of compartments to represent the branched structure of a neuron's dendritic tree. Each compartment represented a constant fraction of the neuron's local space constant (normally 0.1 lambda). Voltages in the interconnected compartments were computed by an implicit method of numerical integration that generated a set of simultaneous difference equations. These were solved iteratively by relaxation (Cooley & Dodge, 1966; Hines, 1984; Smith, 1992). Simulations were run on Silicon Graphics Indigo, Stardent 3000, and Sun 4 workstations. Run time for the complete cone-horizontal model with a 60 × 60 cone array (30,000 compartments, 50,000 synapses) was about 4 h for 100 ms of "neural time."

Cone model

A cone consisted of an outer segment with light-modulated conductance, an inner segment, axon (50 μm length, 1.5 μm diameter), and pedicle. The light-modulated conductance was controlled by a set of difference equations that produced responses similar to those measured in monkey cones, including saturation characteristics but without an explicit adaptation mechanism (Schnapf et al., 1990; Smith, 1992). With a leakage membrane resistance (Rm) in the axon and terminal set at 20,000 Ohm-cm^2, the isolated cone's dark voltage approached −20 mV from a membrane "leakage" potential of −70 mV, and its input resistance was 700 MΩ. When connected to the complete network (i.e. with synaptic connections), the cone input resistance fell to 90 MΩ.

An array of cones with square packing (6-μm spacing, corresponding to the *area centralis* of cat) was interconnected by gap junctions simulated as a linear conductance (Smith, 1992). Each cone was coupled to its nearest eight neighbors (Smith et al., 1986). The cone array was square with a lateral extent of between 40 to 80 cones (240 to 480 μm).

Horizontal cell model

Horizontal cells were given a square dendritic field. A separate dendrite connected the soma to each cone within the dendritic field, and all dendrites were given equal electrotonic length. Type A horizontal cells (HA) received input from 196 cones, whereas type B cells (HB) received input from 100 cones (Wässle et al., 1978*a*; Fig. 3). Leakage resistance was set to 20,000 ohm-cm^2, and membrane capacitance (for cones as well) was set to 1 μF/cm^2. The product of this capacitance and total conductance (membrane leakage and tonic synaptic input) gave a time constant of about 15 ms (see Belgum & Copenhagen, 1988). Two arrays of horizontal cells were constructed with the appropriate cell spacing to give cone coverage factors appropriate for the central cat eye (coverage factor: A = 4, B = 6; Wässle et al., 1978*b*).

Horizontal cells were coupled into syncytial arrays by gap junctions. HA cells were given relatively strong coupling conductances (100 nS, e.g. 1000 connexons) because large gap junctions are known to exist between them (Kolb, 1977). HB cells were given weak coupling (5 nS). Our reasoning was that biocytin injected intracellularly reveals coupling between HB cells but Lucifer Yellow does not (Vaney, 1991, 1993), and that gap junctions are not observed between HB cells by inspection at the EM level (Kolb, 1977).

Synapse model

A synapse was represented by a conductance in series with a voltage source. The conductance was modulated by a function of voltage in the presynaptic terminal (Smith, 1992), based on the model of Belgum and Copenhagen (1988) after Falk and Fatt (1972). The synaptic transfer function was sigmoidal, described by parameters for threshold, slope, and saturation characteristics (Fig. 4, Table 1). Synaptic threshold was defined as the presynaptic voltage that produced a postsynaptic conductance of 2.5% of maximum. The function also included a temporal low-pass filter described by its time constant. The low-pass filters were disabled for the first 20 ms of the simulation to allow the feedback network to stabilize more quickly.

Synaptic connections

Each cone in the simulation provided synaptic input to all horizontal cells whose dendritic fields extended to it (Wässle et al., 1978*a*). Synaptic weight (representing multiple anatomical contacts between cone and horizontal cell, see Kolb, 1974) was set to unity. Since the ratio of HB/HA coverage is about 3/2, the HB array gave stronger feedback to cones than the HA. Neurotransmitter released by cones was excitatory (depolarizing) with a postsynaptic reversal potential in the horizontal cell of −10 mV (Attwell et al., 1987). Synaptic threshold was set to −45 mV (cones) and −50 mV (horizontal cells), suggested by the activation voltage range for calcium channels (Attwell, 1986; see Table 1). Synaptic conductance was set at 200 pS/synapse, which produced a total feedback conductance of 1 nS, roughly the same as the light-modulated conductance in a cone outer segment (Schnapf et al., 1990). Feedback reversal potential (i.e.

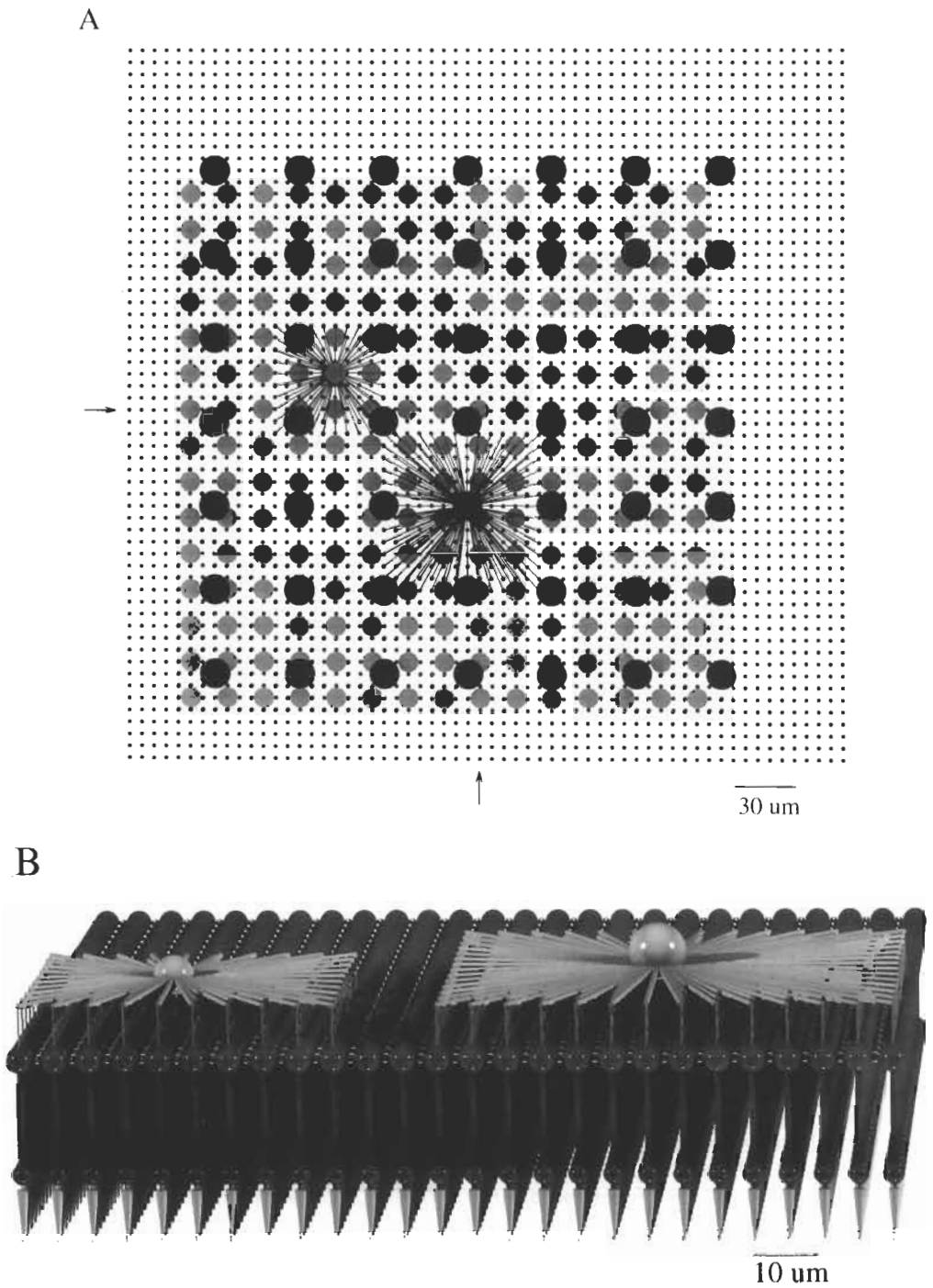

Fig. 3. A: Tangential view of 60 × 60 cone array with one horizontal cell of each type. Type A contacts 196 cones, type B contacts 100 cones. Simplified morphology defines a separate dendrite to contact each cone, and each dendrite is given same electrotonic length. Arrows give row and column of central cone where stimulus was superimposed. B: Radial perspective view of a 26 × 26 cone subset of the network. Cone outer segments are light gray, inner segments, axon and pedicles are dark. Cone–cone gap junctions portrayed as small light spheres between pedicles. Horizontal cells (HB on left, HA on right) contact cones from thin spines that reach vertically from lateral dendrites.

driving potential for the GABA channel in the cone pedicle) was set near −65 mV (Attwell et al., 1983; Skrzypek & Werblin, 1983; but see Burkhardt, 1993). The requirement that the network should not oscillate constrained many combinations of synaptic gain, conductance, and membrane conductance (see below).

Edge effects

Initial simulations revealed both static and dynamic "edge" effects in the responses recorded from initial simulations, e.g. cones near the edge of the array were depolarized at rest from those in the center (Fig. 5). Such edge effects were due to miss-

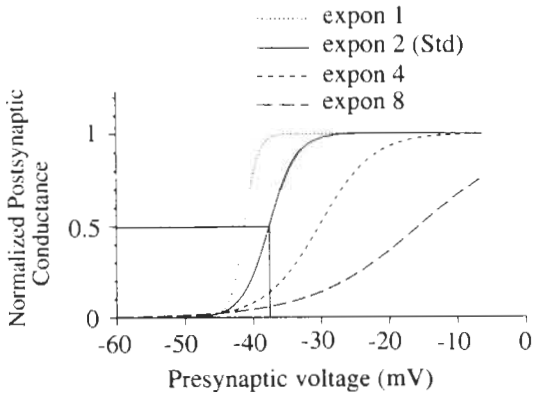

Fig. 4. Synaptic transfer function used in simulation to relate presynaptic voltage to postsynaptic conductance. An exponential release function of the form $Trel = \exp[(V - V\text{thresh})/\text{expon}]$ produced varying gains when supplied with different values for "expon" (different traces). Note that all curves cross at the threshold of −45 mV, the point at which the conductance is 2.5%. The released transmitter (*Trel*) was applied to a Michaelis-Menton saturation function, $Tsat = Trel / (Trel + 1)$, to produce the overall S-shaped function. Solid line shows that a presynaptic voltage of approximately −37 mV relates on the "expon 2" plot to a normalized postsynaptic conductance of 0.5, the point at which the synaptic gain curve is most linear.

ing feedback connections to cones within the array from horizontal cells outside the array. To compensate, we added extra feedback synaptic connections to those cones near the edge so they received same number as the central cones. This improved their resting potentials (Fig. 5), but other edge effects remained in the network's response to a stimulus.

To identify such dynamic edge effects, we compared the cone receptive fields of several models differing only in the network's extent. Arrays of 40 × 40, 60 × 60, and 80 × 80 were run and the resulting cone receptive fields compared (not illustrated). The receptive-field centers were identical but the surround of a smaller network's receptive-field profile was artifactually deep near the network edge. These artifacts were not compensated for by adding synapses at the edge. However, the surround computed from the 60 × 60 array was essentially identical to that of the 80 × 80 array and the effect on the surround of compensatory synapses was nearly undetectable.

Stimuli

The main stimulus used for mapping receptive fields was a small spot (1 μm diameter) convolved with an optical blur function. To generate the blur function, we averaged the results of Wässle (1971) and Robson and Enroth-Cugell (1978), normalized for a cat eye with a 4-mm pupil, and approximated it as a Gaussian point-spread function of 22-μm diameter (at 1/e peak). To this we added an approximation of the pronounced "tails" caused by scattered light (Robson & Enroth-Cugell, 1978). The spot was presented as a brief flash (1 ms) centered in the network. The peak intensity at the cones' outer segments was 5e6 photons/μm²/s (~10,000 photons/cone), just below saturation (Fig. 6). In other cases, the stimulus was a 22-μm bar (Fig. 7b) or a 150-μm spot (Figs. 6 and 15), blurred with the same 22-μm point-spread function.

Table 1. *Standard parameters for simulation*

Cones	
Membrane	
Light-modulated conductance	1.4 nS, −8 mV driving force
Rm	20,000 Ohm-cm²
Ri	200 Ohm-cm (Spruston & Johnston, 1992)
Cm	1 μF/cm²
Driving force for *Rm*	−70 mV
Gap junction conductance	100 nS
Conductance from Hz cells	1 nS/Hz cell/coverage factor
Feedforward synapses	
Neurotransmitter action	Depolarizing
Gain parameter	2 mV/e-fold increase
Threshold	−45 mV
Reversal potential	−10 mV
Time constant	0.4 ms
Conductance	100 pS
Morphology	
Outer segment	Sphere, diameter 16 μm for capacitance
Axon	Length 50 μm, diameter 1.5 μm
Pedicle	Sphere, diameter 5 μm
Number of horizontal cell feedback synapses:	
Coverage factor, HA	4
Coverage factor, HB	6
Topology	
Cone array size	60 × 60, square
Cone spacing	6 μm
Horizontal cells	
Membrane	
Rm	20,000 Ohm-cm²
Ri	200 Ohm-cm (Spruston & Johnston, 1992)
Cm	1 μF/cm²
HA gap junction conductance	100 nS
HB gap junction conductance	5 nS
Conductance from cone synapse	200 pS/spine
Feedback synapses	
Neurotransmitter action	Hyperpolarizing
Gain parameter, HA	2 mV/e-fold increase
Gain parameter, HB	2 mV/e-fold increase
Threshold	−50 mV
Reversal potential	−67 mV
Time constant	20 ms
Conductance	200 pS
Morphology	
Size of HA dendritic tree	84 μm, square
Size of HB dendritic tree	60 μm, square
Simulated Hz cells contact all cones within dendritic field.	
Number of cones contacted, HA	196
Number of cones contacted, HB	100
Topology	
Coverage factor, HA	4
Coverage factor, HB	6
Stimulus	
1-μm spot, convolved with 22 μm (diameter at 1/e) Gaussian point-spread function.	

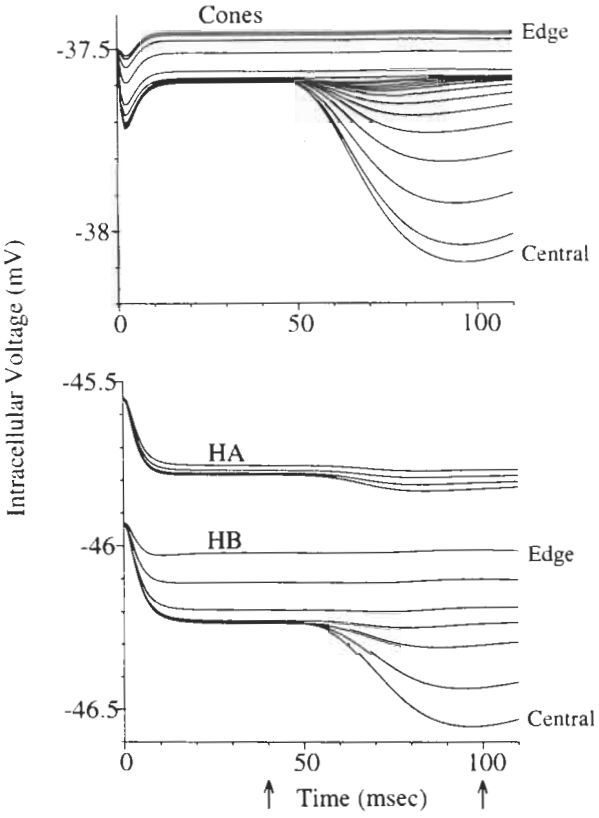

Fig. 5. Time plot of voltage responses in the network. Responses taken from cones and type B horizontal cells along a radius to produce receptive-field space plots (Figs. 7–14). Records were taken from every cone along the radius from 0 to 60 μm and thereafter from every other cone (i.e. spaced 12 μm apart). Responses labeled "Central" and "Edge" are from cells, respectively, at center and edge of network. Simulation starts with precomputed approximate resting potentials. Network stabilizes for 20–30 ms, light flash at 40 ms (1 ms, 10,000 photons/cone, at first arrow), and response recorded at 100 ms where it reaches maximum (second arrow). A correction for edge effect was included by adding feedback synapses that would have originated in horizontal cells outside network.

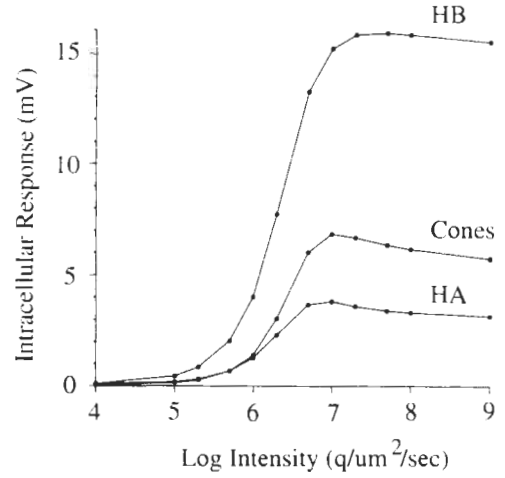

Fig. 6. Intensity response of cones and horizontal cells in the simulated network. Stimulus was a 150-μm spot centered on the network flashed for 100 ms on a background of 1000 quanta/μm^2/s. Each point represents the difference between peak and resting voltages of the central neuron of each of the three cell arrays. HB cell has high gain because its receptive-field diameter approximates stimulus diameter. Although HA cell has similar synaptic input from cones, it has lower gain because its receptive field is wide due to electrical coupling. The slight decrease in response of all three cell types at higher intensities is due to temporal properties of feedback.

Receptive-field measurement

A receptive field is normally mapped *in vivo* by recording the response of a neuron to a stimulus moved across space. However, to compute a simulated receptive field in this manner would be extremely costly in computation time. Instead, we centered the stimulus on the network and recorded simultaneously the responses of many cones and horizontal cells across a radius of the network. A plot of peak responses of these cells plotted against their spatial locations was equivalent to the receptive field of one cell. Thus, receptive fields of all three cell types were measured simultaneously from the response to a single flash (see Fig. 8). Since the stimulus in most cases was a radially symmetric spot, the receptive field had approximate radial symmetry and could be described in the form of a Bessel function of radius. However, since a Bessel function approaches the corresponding one-dimensional exponential function (measured with an extended bar) as radius increases, we informally describe slowly decaying receptive-field profiles as "exponential" in form to differentiate them from the quickly decaying "Gaussian" form (see Results).

Tuning the network parameters

After initial calibration, the network parameters were adjusted to give a cone receptive field that approximated in amplitude and spatial extent a difference-of-Gaussians template derived from the convolution model (Fig. 7a; see Smith & Sterling, 1990). Although the network when tuned in this manner reasonably matched the template, there were several degrees of freedom: membrane resistance, coupling conductances, synaptic conductance, gain, and threshold. Within this parameter space many tradeoffs were possible. For example, the effect on the normalized cone receptive field of small increases in feedback gain were equivalent to decreases in cone coupling (Fig. 7c). Since there was no way to decide which particular combination was biologically correct, we simplified comparisons by settling on a set of parameters that matched ganglion cell physiology as a standard "central set" (Table 1). Our goal was to assess which parameters are both sufficient and necessary to generate a difference-of-Gaussians cone receptive field.

In most cases parameters were constrained, sometimes in several ways, by biophysical limits or by the function of the circuit. Several important constraints were that:

1. The resting potentials should be appropriate, for example, within the range of -10 to -70 mV.

2. The network should not oscillate. This limited overall voltage gain for the loop to less than 1. This relation limited feedback gain to the inverse of feedforward gain:

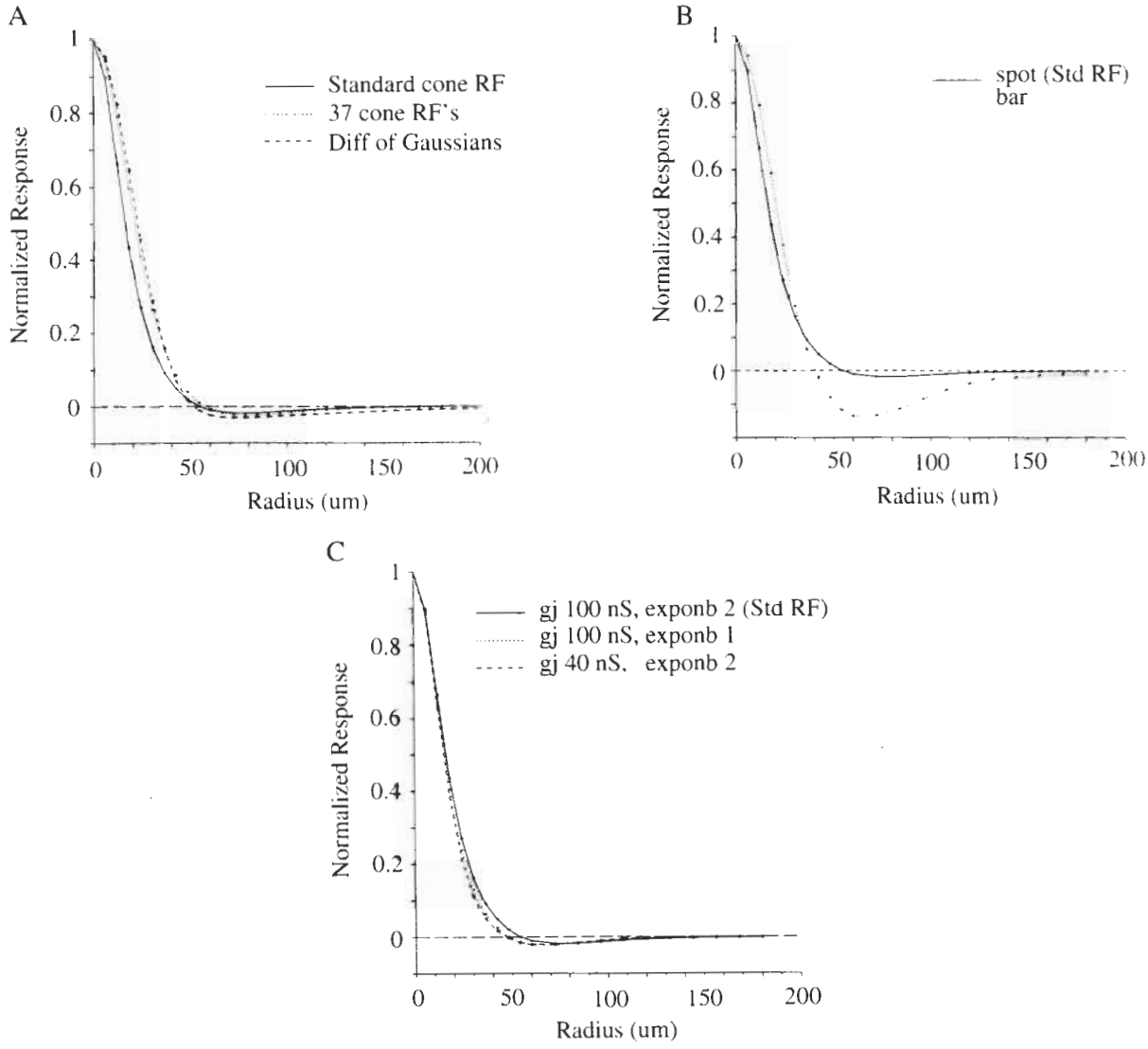

Fig. 7. A: Cone receptive field computed from standard network parameters compared to the convolution of 37 such cone receptive fields that constitutes the beta ganglion cell receptive field (see Smith & Sterling, 1990). Beta receptive field is plotted as a difference-of-Gaussians ($Ks/Kc = 0.04$, $Rs/Rc = 5$). The effect of the convolution is to broaden center slightly, giving it a more Gaussian profile, and to deepen surround. Note that the convolution of 37 cone receptive fields accounts fairly well for the shape and extent of the beta cell receptive-field center. The convolution is shallower in the surround than the beta cell receptive field, and this is consistent with additional inhibition onto bipolar dendrites (Vardi & Sterling, 1994), bipolar cell axon terminals, and beta cell dendrites (Freed, 1992; Hughes et al., 1991). B: Cone receptive field measured with spot (standard parameters) and 22-μm bar. Surround plotted with bar is deeper relative to center because surround is much larger than center so bar overlaps to a greater extent. However center sizes are nearly identical. C: Cone receptive field from standard parameters (as in A) *vs.* two non-unique parameter combinations. The effect of halving cone gap junction coupling (gj 40 nS) is similar to the effect of doubling HB feedback gain (exponb 1).

Loop gain = Forward gain * Feedback gain

Constraint: Loop gain < 1

Therefore: Feedback gain < 1/Forward gain

Since each neuron's membrane properties defined an intrinsic temporal low-pass filter the gain constraint affected mainly responses at low temporal frequencies.

3. Feedforward gain (i.e. the ratio of cone to horizontal cell responses) was constrained to be in the range of 1–2 with full-field flash (Belgum & Copenhagen, 1988).

4. The ratio of synaptic to membrane conductance in the horizontal cell contributes to feedforward gain, and the range of these conductances was limited by biophysical assumptions. Input resistance of a cone affected feedback gain and input resistance varied with membrane properties and degree of electrical coupling in the cone network.

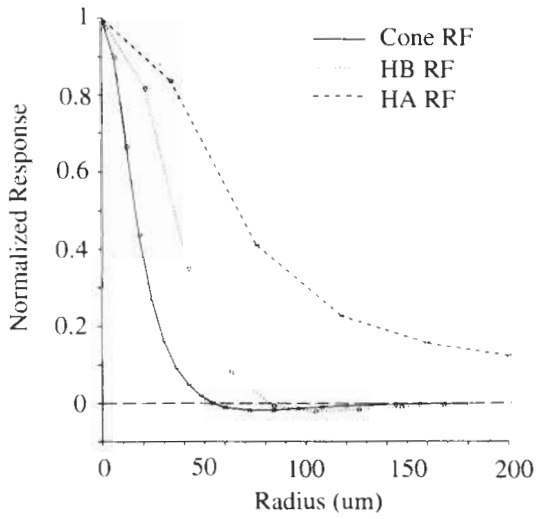

Fig. 8. Receptive fields of the cone, HA, and HB cells with standard network parameters. Note that HA receptive field decays exponentially with radius but HB has surround which truncates its center relatively sharply.

5. The cone synapse should operate around the midpoint of its input/output function. This is necessary for the cone to impart equal gain to signals greater than and less than the mean level.

Results

Summary of simulation

We selected for simulation a square array of 60 × 60 cones which was large enough to capture the function of cone center and surround without much edge effect (see Methods). The light stimulus was usually a small spot, presented to the center of the array through a convolution filter that simulated optical blur (see Fig. 1). The simulation included arrays of horizontal cells (7 × 7 type A, 15 × 15 type B; Fig. 3) and were interconnected with the cone array by reciprocal synapses. Receptive fields were measured by recording from multiple sites in each array the responses to a single light flash.

Resting potentials

As an isolated neuron, the cone sits at a dark potential of about −20 mV, and the horizontal cell sits near −70 mV. When the complete network is turned on, their synaptic interactions within 20 ms of "neural time" produce a stable cone potential of −37 mV and horizontal cell potentials of −45 mV (Fig. 5). Resting potentials of cones and both types of horizontal cells are uniform (to 0.2 mV) across the network except near the edge. As noted in Methods, the network includes compensatory feedback onto the cones near the edge, but this method left vestiges of depolarization in the cones and HB cells near the edge.

Resting potentials were affected by several parameters including synaptic threshold, synaptic gain, synaptic conductance, and membrane resistance. For most of these combinations, the cone array rested between −44 and −35 mV, and horizontal cells rested between −50 and −30 mV, consistent with published records (Foerster et al., 1977; Steinberg, 1969). With high values of synaptic gain and/or input resistance (see Methods), resting potentials were unstable (i.e. they oscillated).

Light responses

When a small spot of light (1 μm diameter, but with blur added) is flashed (1 ms) at the center of the cone array, the cones and horizontal cells hyperpolarize, the response peaking at 60 ms (Fig. 5). The peak responses vary across the cone array, and these were used to plot receptive fields. Responses across the HA array are low in amplitude and essentially uniform, but across the HB array they are larger and nonuniform. This suggests an important difference between the two types that we explored further with stronger stimuli.

A large spot covering the full dendritic field of the central horizontal cells (Figs. 15a and 15b) evokes in all three cell types a marked transient-plus-sustained hyperpolarization with a modest poststimulus depolarization. This pattern resembles recordings from mammalian horizontal cells (Steinberg, 1969; Nelson, 1977; van de Grind & Grüsser, 1981; Lankheet et al., 1990; Bloomfield & Miller, 1982; Dacheux & Raviola, 1982).

A plot of response *vs.* intensity from the network shows the response of an HB cell is greater than either the cone or HA to a spot that matches the HB receptive-field extent (Fig. 6). Simulated light responses showed the "S" shape typical of published responses (Nelson, 1977; Bloomfield & Miller, 1982; Lankheet et al., 1991) except that the range of linear response in the simulated network was narrower. This difference may be related to the fact that the transduction element of the simulated cone, although designed to produce a realistic response to different intensity flashes (Smith, 1992), did not possess "biochemical adaptation" that is thought to occur in the outer segments of cones (Tranchina et al., 1991).

Receptive fields

The cone receptive field mapped from the standard network has a relatively broad, Gaussian-like center whose space constant (~25 μm) is more than twice the diameter of the optical point-spread function (Figs. 7, 8, 9, and 11). The receptive field also has a Gaussian-like surround. The convolution of 37 such receptive fields appropriately spaced matches the beta ganglion cell's center and surround Gaussians (Fig. 7a) except that the surround produced is somewhat lower in amplitude. This is consistent with evidence of additional sources of lateral inhibition on the pathway to ganglion cells, including GABA input to the bipolar dendrites (Vardi & Sterling, 1994), bipolar axon (Pourcho & Owczarzak, 1989; Suzuki et al., 1990; Yeh et al., 1990), and ganglion cell (Freed, 1992). When mapped with a bar, the receptive-field surround deepens but the center diameter is almost unchanged (Fig. 7b). This is consistent with actual receptive fields of ganglion cells plotted with narrow bars (Cleland et al., 1979; see Smith & Sterling, 1990).

In one sense, this relatively broad, center-surround cone receptive field is not a *true* "result" because, as noted, the standard values in the model were deliberately chosen to produce it. Furthermore, the parameter values that produce this receptive field are not unique. For example, an essentially identical result is obtained when the cone coupling conductance is reduced while the HB gain is increased (Fig. 7c). On the other hand, the center-surround cone receptive field *is* a "result" because the parameter values are all plausible and the network is sufficient

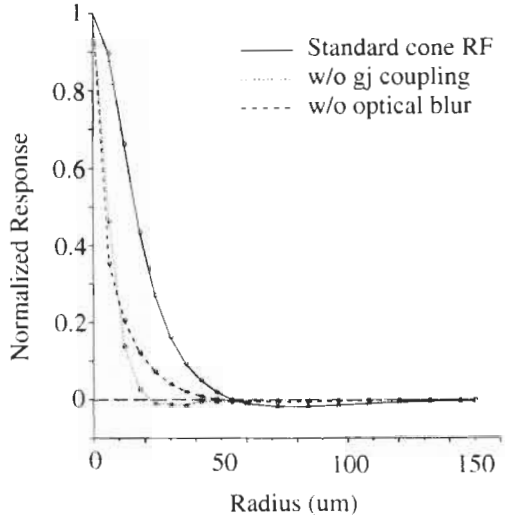

Fig. 9. Standard cone RF compared to cone RF without coupling or without optical blur. Main effect of gap junctions is to broaden skirt of center. Without coupling surround is weak because center response is substantially smaller in diameter than horizontal cell receptive field. Smooth central dome (1/e radius, 11 μm) in receptive field generated by Gaussian optical blur without coupling (dotted line) is not visible in plot because receptive field was sampled at 6-μm intervals in adjacent cones (see "Receptive field measurement" in Methods).

to produce it. Furthermore, the same values reproduce other important features such as details of horizontal cell receptive fields that were *not* tuned into the model.

Horizontal cell receptive fields

The HA receptive field from the standard network has a skirt of approximately "exponential" form as would be expected from gap junction coupling (Fig. 8; Lamb & Simon, 1976). The space constant is about 100 μm, almost three times greater than the radius of the dendritic field (~42 μm in the simulation), and there is no surround. This is similar to the actual receptive fields reported by Nelson (1977) and Lankheet et al. (1990). Under some conditions (e.g. when mapped by spot displacement), however, cat and rabbit HA receptive fields are much larger, on the order of ten times greater than the dendritic reach (Lankheet et al., 1990; Bloomfield & Miller, 1982).

The HB receptive field appears more Gaussian than exponential and has a smaller space constant (~50 μm) (Fig. 8), about 50% greater than the dendritic reach. The HB receptive field also exhibits a definite inhibitory surround. This is an emergent feature of the network that has not been reported for mammalian cells corresponding to the HB. However, an inhibitory surround has been demonstrated for the homologous narrow-field horizontal cells in turtle (Piccolino et al., 1981), and also in salamander (Skrzypek & Werblin, 1983).

Function of components in circuit

Origin of the receptive-field center

Cone coupling and optical blur both contribute to the standard cone receptive field (Fig. 9). When optical blur is omitted from the simulations, the cone center has a sharp peak due to exponential decay from cone-cone coupling. The inclusion of optical blur widens the central peak into a smooth dome. In a simulation with optical blur and cone-cone coupling but without horizontal cells, the central dome decays exponentially beyond the radius of optical blur (11 μm) (Fig. 10).

Cone-cone coupling

The two main effects of cone-cone coupling are to widen the cone receptive-field center (due to lateral spread of current) (Figs. 10b and 11b), and to reduce its amplitude (lateral path of current shunts the cone response) (Figs. 10a and 11a). In the complete network, the effect of increased coupling in the normalized cone receptive field is to expand the receptive-field center and reduce the proximal surround (Fig. 11b). Removal of cone-cone coupling narrows the center to match the optical blur function, increases the absolute center amplitude, and reduces surround strength relative to the center (Fig. 11b).

Horizontal cell coupling

The strength of electrical coupling between horizontal cells modulates their receptive-field amplitudes and diameters (Fig. 12).

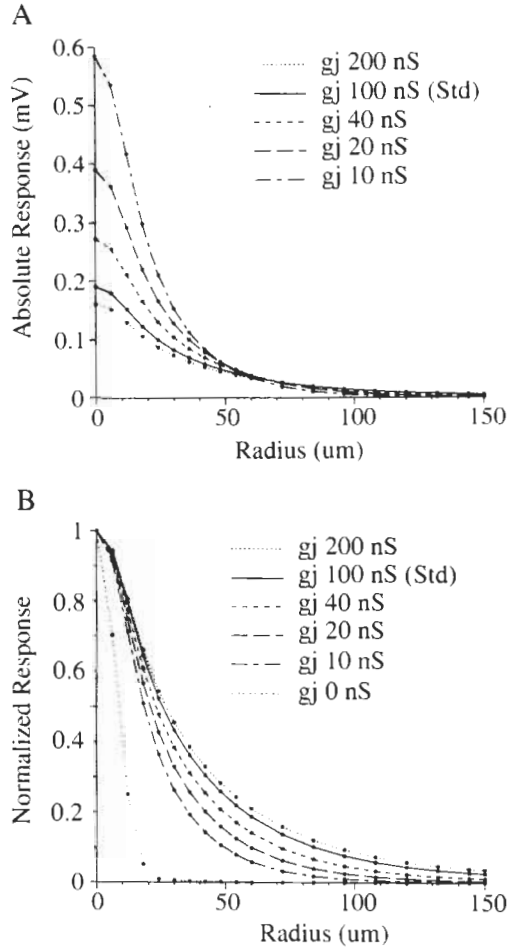

Fig. 10. Effect of different cone-cone gap junction conductances on cone receptive field in network without horizontal cell feedback but including optical blur. A: Gap junction coupling reduces amplitude of response due to lateral current spread. B: Normalized plot; coupling produces exponential-type receptive field whose space constant varies with conductance.

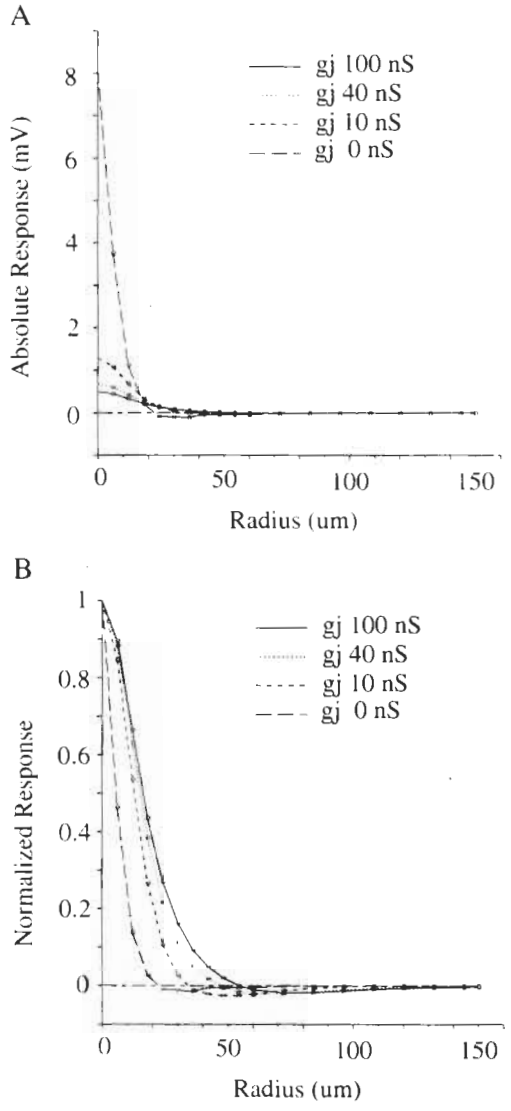

Fig. 11. Contribution of cone coupling and optical blur to standard cone receptive field. A: Amplitude of cone response. Over a wide range of coupling, responses reduced to millivolt range. B: Response normalized to emphasize lateral extent. Modulation of coupling affects center shape and proximal surround amplitude.

Increased coupling reduces the peak amplitude and expands the receptive-field center. Over a wide range of coupling strengths, the HB has an antagonistic surround which originates in the cone surround generated by neighboring horizontal cells (Figs. 12c and 12d). When HB cells are given strong coupling, their receptive-field center expands at the expense of the surround, producing a receptive field similar to the HA (Figs. 12c and 12d). A further increase in HB coupling eliminates its surround but this happens only at levels of coupling where the HB receptive-field diameter approaches that of the HA.

Horizontal cell feedback gain

A perturbation in feedback gain from either HA or HB modulates its influence on the cone receptive field. For example, an increase in HB feedback increases the depth of the cone's proximal surround (Fig. 13), and an increase in HA feedback increases the depth of the distal surround. In this respect, the action of an horizontal cell type on the cone receptive field is related to the horizontal cell's receptive-field profile (see Fig. 8).

However, a perturbation in synaptic gain produces an additional effect on the cone receptive field not directly proportional to the horizontal cell's receptive-field profile. Synaptic gain controls resting potentials throughout the network which induce nonlinear effects (see "Balance of feedback" below). For example, a decrease in HB feedback gain increases the distal surround amplitude (Fig. 13), and a decrease in HA feedback increases the proximal surround.

Entirely removing one of the horizontal cell types amplifies the effect of a change in feedback gain. Without HA feedback, the distal surround of the cone is reduced and the near surround strengthened. Without HB (HA restored) the proximal cone surround is reduced and the distal surround strengthened (Fig. 14). In both cases the reduction in feedback allows the cone resting potential to depolarize significantly towards the driving potential of the light-modulated outer segment conductance. This "saturation" effect reduces the cones' light response, so to demonstrate the spatial differences in this case, we partially compensated for the saturation by increasing the remaining feedback two-fold. When both horizontal cell types are removed (Figs. 10 and 14), the cones depolarized (to −14 mV, not illustrated), reducing the amplitude of light responses (compare Fig. 10a with Fig. 11a). This suggests one function for horizontal cell feedback might be to maintain the cone resting potential in a non-saturated state (see Discussion).

Modulating gap junction coupling between either HA or HB affects cone receptive-field profiles throughout the network but does not affect resting potentials. For example, an increase in HB coupling directly reduces the HB receptive-field amplitude and increases the diameter (Figs. 12c and 12d). These effects in turn reduce the cone's proximal surround and increase its distal surround (not illustrated).

The action of negative feedback

The cone resting potential in the network is hyperpolarized from the resting potential of an isolated cone due to negative feedback. Depending on the synaptic loop gain, the feedback tends to "clamp" the resting potentials of both cone and horizontal cell to several millivolts depolarized from their respective synaptic thresholds (see Figs. 5 and 15 and Table 1). An hyperpolarizing perturbation in the cone decreases transmitter release and hyperpolarizes horizontal cells, which in turn decreases the horizontal cells' transmitter release and causes a depolarization of the cone, opposing the original perturbation. Thus, negative feedback maintains a nearly constant synaptic activation.

Nonlinearities in synaptic transfer functions affect the operation of the feedback circuit. Since synaptic gain is dependent on the presynaptic voltage level, gain tends to be low at hyperpolarized and depolarized voltages, and high at intermediate voltages. An hyperpolarization of the cone pedicle reduces gain in the forward cone → horizontal cell synapse because the slope of its transmitter release curve diminishes at threshold (Fig. 4). Such a modulation of gain can arise from either an injected current or a cone's response to light (e.g. see Fig. 15). The overall loop gain is dependent on the "operating point" in a complex way because several factors (stimulus, synaptic gains, other

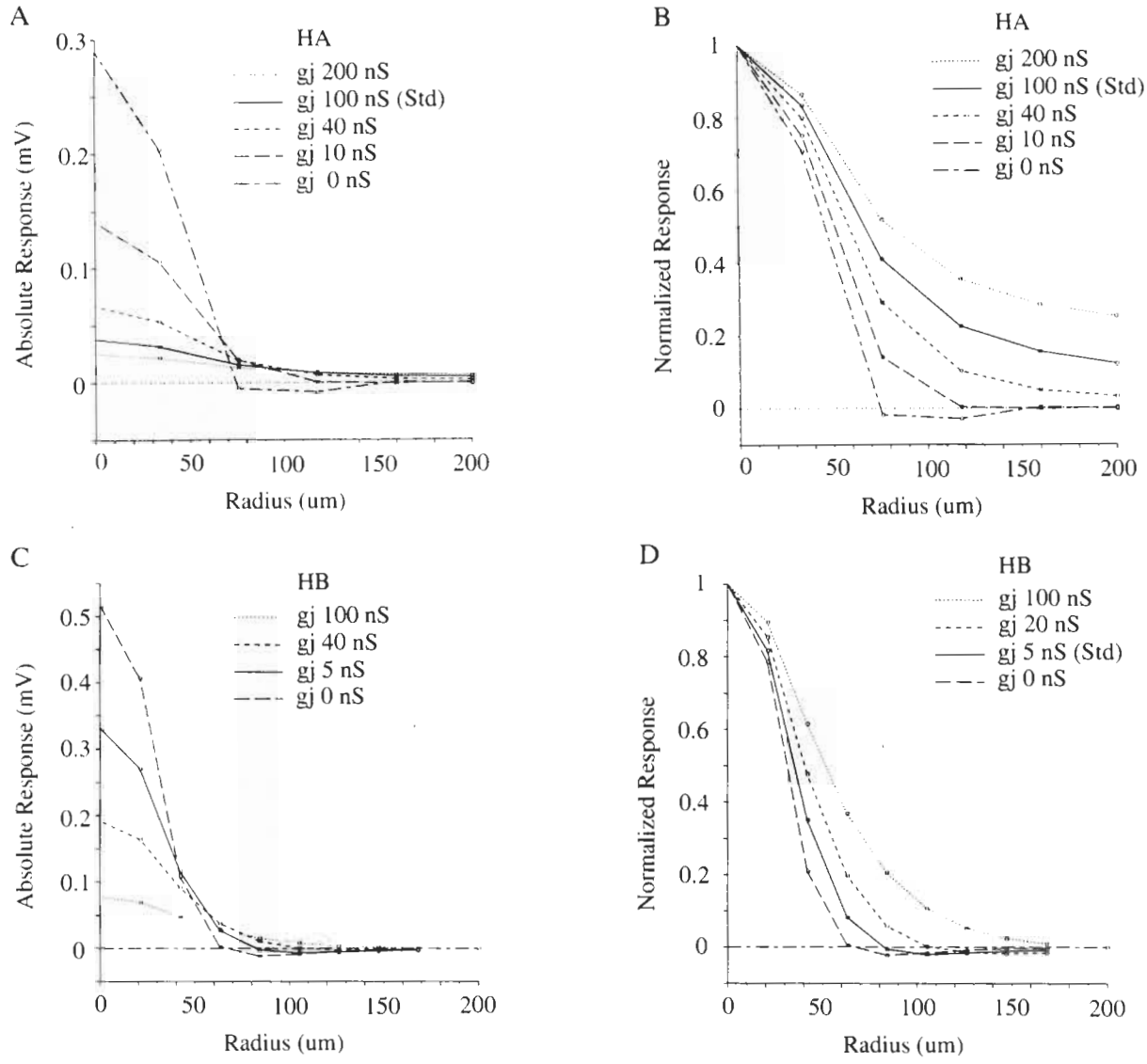

Fig. 12. Effect of horizontal cell coupling on HA and HB receptive fields. A: HA response amplitude. Increasing coupling conductance reduces amplitude as in cone array. B: HA normalized responses. Receptive field is exponential with large coupling conductances. C: HB response amplitude. For small conductances (<100 nS), an obvious surround appears. D: HB normalized responses. Large conductances give exponential receptive field, small conductances give more Gaussian-like receptive field.

membrane conductances) control presynaptic voltages (see Methods).

Effect of feedback on gain for two signals

A further complexity is introduced into the cone-horizontal feedback circuit because its neurons reduce their transmitter release with light. During a light response, negative feedback tends to decrease the cone's chloride conductance. The decrease in conductance disinhibits the cone, opposing the original hyperpolarization to light, but under some conditions it also increases the gain for light stimuli. When the change in shunt conductance causes a large enough increase in synaptic gain at the cone pedicle, it leads to instability (e.g. Fig. 15b).

Such an effect is fairly direct when there is one stimulus, because negative feedback can only oppose it. However when two stimuli are given, their feedback effects tend to interact. For example, a depolarizing current injected into all cones (e.g. mimicking the effect of turning off a rod stimulus) depolarizes the cones and horizontal cells, which increases feedback and also may increase loop gain. However, the increased feedback also shunts the cone, decreasing its input resistance, and decreasing its tonic response to light (Figs. 15a and 15b). This "positive feedback" effect is similar in sign and magnitude to the "suppressive rod-cone interaction" measured in horizontal cells (Pflug et al., 1990; Lankheet et al., 1993), therefore a similar feedback mechanism may be responsible.

Effect of resting potentials

Resting potentials are an important determinant of network function because they control synaptic gain. When resting poten-

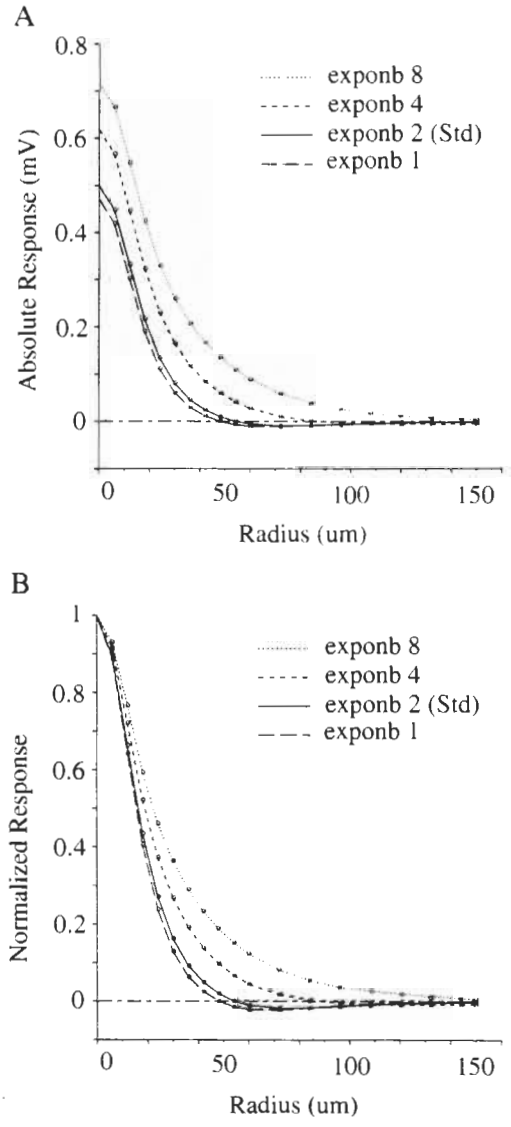

Fig. 13. Effect of synaptic feedback gain on cone receptive field. Standard set of parameters, except the "expon" parameter ("mV / e-fold increase in gain") for HB horizontal cells varied from 1 to 8. A: Absolute amplitude plot. Reducing gain from 1 to 8 increases amplitude of cone center response but less dramatically than reducing cone coupling. B: Normalized responses from A. Reduced gain reduces proximal surround and increases distal surround. At intermediate gain, (expon = 4) effect of HB array lessens and HA takes over to generate wide shallow surround.

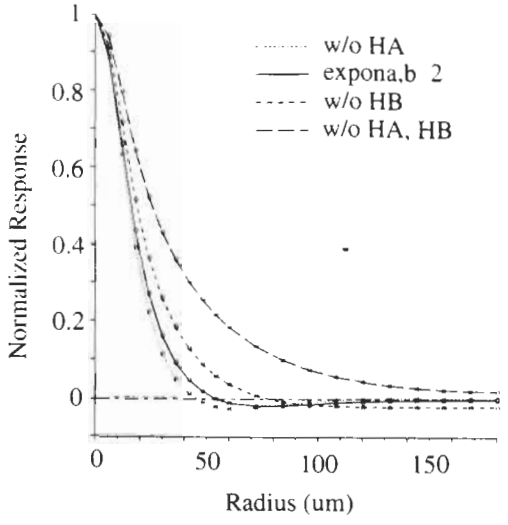

Fig. 14. Effect of removing HA and/or HB horizontal cell feedback on cone RF. Conductance of the remaining synaptic feedback was doubled to prevent depolarization and saturation of cone response. When only HA is removed, the distal surround approaches zero amplitude. When only HB is removed, the proximal surround reverts to exponential-type center. When both types are removed, surround disappears completely (see Fig. 9).

tials in the network lie in the central linear portion of both feedforward and feedback synapses' input range (i.e. 5–10 mV above threshold), synaptic gains are maximal and the network loop gain behaves in an "additive" fashion, i.e. a reduction in synaptic gain (or an hyperpolarization of resting potential) reduces loop gain in the network.

However, when resting potentials are offset from the middle linear portion of the transfer curve (e.g. hyperpolarized due to increasing the synaptic feedback conductance parameter), synaptic gains are less than maximal. In this case the loop gain of the network is affected by negative feedback, i.e. a reduction in synaptic gain causes a shift in resting potential that tends to restore the original level of gain (not illustrated).

Dynamic balance of feedback

To discover the effect of nonlinear feedback, some simulations were run with resting potentials near synaptic threshold but with higher synaptic conductance to maintain loop gain. In this circumstance, negative feedback tends to reduce HA and HB feedback gains (by hyperpolarizing the entire network), so gain is dynamically controlled. Cone center and surround space constants are not controlled by a preset level of feedback but by the balance between HA and HB feedback gains (Fig. 16). The explanation for this is that both circuits include the same cone pedicle and synapse. An increase in synaptic gain from HA to the cone terminal causes the cone terminal to hyperpolarize, which opposes the original increase in feedback. The cone hyperpolarization, however, also affects HB, nonlinearly reducing its influence (i.e. gain) on the cone.

Discussion

The model's standard set of parameters reproduces the basic properties known from intracellular recordings in cat, including stable resting potentials of the appropriate magnitude, light responses of the appropriate amplitude and time course, and the appropriate receptive field of the HA horizontal cell (Steinberg, 1969; Nelson, 1977; Lankheet et al., 1990). The model also produces other properties anticipated from studies on other species: an HB receptive field smaller than the HA and with an inhibitory surround (Piccolino et al., 1981), and for a wide variety of parameter values, a broad center and antagonistic surround in the cone (see Hsu & Smith, 1994).

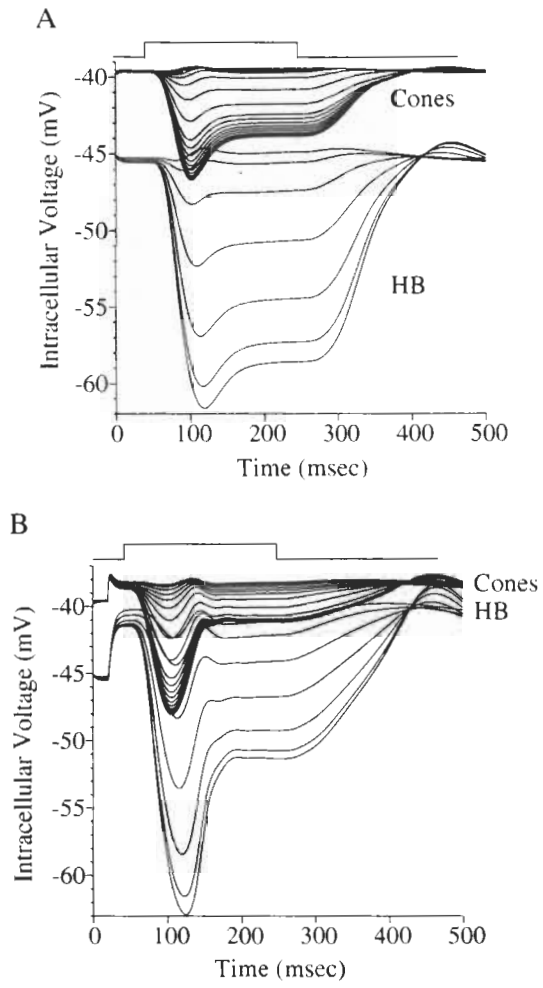

Fig. 15. Response of the network to large spot (150 μm) of 200-ms duration. Standard parameters, except feedforward conductance 200 pS/synapse that hyperpolarizes cones through feedback. Records from 21 cones and 13 HB horizontal cells taken along a radial line from center; central responses most hyperpolarized (see Fig. 5). Cones rest at −39 mV, horizontal cells at −45 mV. Hyperpolarizing "nose" is due to delay in feedback loop, which includes feedforward synapse delay, horizontal cell time constant, and feedback synapse time constant (20 ms). Biphasic response in cones near edge results from current spread through cone gap junction coupling added to delayed feedback from horizontal cells. A: Light stimulus only. B: Effect of 20 pA current injected into each cone, starting at 20 ms. Nose is increased but tonic response to light is decreased due to feedback effect of injected current. Slight ringing occurs at end of nose in feedback because feedback loop gain is greater. When gain parameters (feedback or feedforward) set slightly larger, entire network becomes unstable (not illustrated).

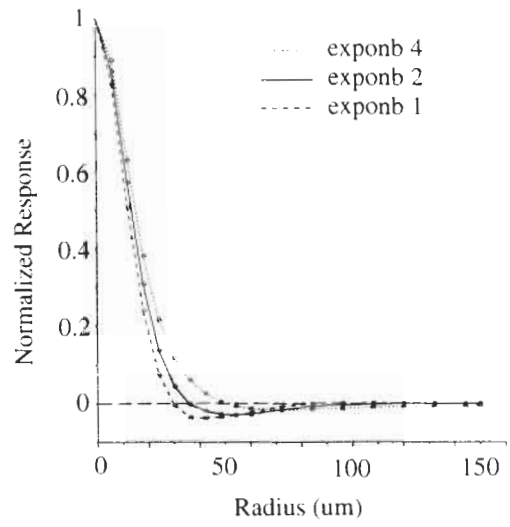

Fig. 16. Effect of setting gain parameters so resting voltage is in nonlinear "toe" region of synaptic transfer curve. With high HB feedback gain (exponb = 1), cone surround is narrow and deep, corresponding well with HB receptive field. Lower HB feedback gain causes cone surround to be "HA-like", i.e. shallow and wide.

Our simulations suggest several conclusions regarding the assembly of the cone receptive field. (1) A broad cone receptive-field center originates in optical blur and cone-cone coupling because when either of these factors was omitted from the simulation, the cone center shrank; (2) the cone surround is related to the HA and HB receptive-field amplitude and extent, and to the strength of feedback, and (3) the cone receptive field's approximate "difference-of-Gaussians" shape (i.e. broad dome-shaped center decaying rapidly with radius to weak wide surround) evidently is an emergent property of the network.

A major reason for amplifying the visual signal at an early stage in its pathway is likely to be less vulnerability to noise at later stages. The first synapse from the cone pedicle to bipolar cells likely has relatively high gain for this reason (Belgum & Copenhagen, 1988). However, high gain has a consequence: the synapse saturates (i.e. it distorts the signal) on the maximum and minimum ends of its range (Fig. 4). As a result, the range of voltage over which neurotransmitter release can be usefully modulated is relatively narrow (Belgum & Copenhagen, 1988; Attwell, 1986; Werblin, 1971).

Function of the cone surround

Our simulations suggest that a surround for the cone pedicle would perform two distinct functions to maintain high gain for the cone signal. First, the pedicle's light-driven signal is opposed by horizontal cell feedback, which disinhibits the cone pedicle, tending to drive the pedicle voltage towards its initial resting voltage, near the "middle" of the synaptic transfer function where gain is highest (Fig. 4; see Laughlin et al., 1987; Burkhardt, 1993). This conclusion follows from the result that the cone's weak but wide antagonistic surround (Figs. 5, 13, and 14) originates in negative feedback from horizontal cells. Subtracting the horizontal cell signal from the light signal tends to eliminate "redundant" (i.e. transmitted by more than one cone) low spatial-frequency components of cone signals (Srinivasan et al., 1982). Such a system allows signals from bright and dark objects to be coded equally well by the synapse (Fig. 4), and reduces distortion.

The second function performed by negative feedback from the surround is related to transfer of the cone's signal from the outer segment to pedicle. When some cone outer segment channels close in response to light (E_{rev} −10 mV), negative feedback closes some of the pedicle's GABA-sensitive chloride channels (E_{rev} −67 mV) in response. These conductances of the cone can

be approximated as a resistive voltage divider and the small-signal response of such a circuit is optimal when the resistances are equal, i.e. when the voltage rests at the middle of its range (see Appendix), near to the voltage (−38 mV) maintained by negative feedback (Figs. 5 and 15). Therefore negative feedback also tends to maintain optimal transfer of low-contrast signals from outer segment to pedicle. Such a tonic chloride-based feedback would imply some sort of chloride pump to maintain osmotic balance inside the cone.

Function of the two horizontal cell types

The fact that horizontal cells are not heterotypically coupled (Kolb, 1977; Vaney 1993) suggests that their receptive fields might differ in some way. Indeed, our simulations suggest that while both types of horizontal cell are involved in computing the cone's surround, they perform slightly different functions because the extent of their coupling may differ. The HA, being large and well coupled, has a large receptive field (>200 μm, see Lankheet et al., 1993). In our simulations the HB, being smaller and not well coupled, has a small receptive field (100 μm) and a more local effect (Figs. 8, 12, and 14). In simulations with only one horizontal cell type, either one alone produced an exponential receptive-field surround in the cone (Fig. 14), but the action of both types in the complete network was more complex.

Our results suggest that the two types of horizontal cell together produce a surround in the cone that neither could produce alone. Although we do not know the exact properties of HA and HB feedback onto cones, our simulations show that tuning their feedback gains would modify the cone surround profile but only over the range in which both types influence the cone (Figs. 13 and 14). A large disparity in gain between HA and HB would imply that one of them would have essentially no function in the circuit. Therefore it seems likely that both HA and HB feedback contribute to the surround, which would thereby contain a mixture of wide and narrow components, reminiscent of a Gaussian (Figs. 8 and 14). Thus, it appears that the function of the two types of horizontal cell is to fashion a Gaussian-like surround in the cone. Since the dome shape of a receptive-field center is optimal for increasing signal/noise ratio (Tsukamoto et al., 1990), it is likely that a similar shape is optimal as well for the surround.

Modulation of surround

Another possibility is that a differential modulation of synaptic gain in the two types could be important for the circuit's function. If the circuit were modulated (e.g. by light through the action of dopamine) so that feedback from one type was weak and the other strong, the weak one would be effectively eliminated from the circuit because of nonlinear properties of the feedback, and the surround from the strong one would remain. Thus, the two horizontal cell types might provide dynamic control over spatial properties of the cone surround.

Lankheet et al. (1990) found HA receptive-field size to vary depending on stimulus configuration and intensity. They found that (1) low intensity or spot displacement measurements (which minimize light falling in a neuron's receptive field) gave larger receptive fields, and (2) high intensity or spot size measurements gave smaller receptive fields. In our simulations (not illustrated) as well as physiological recordings in lower vertebrates (e.g. Belgum & Copenhagen, 1988), illumination causes an increase in horizontal cell membrane resistance, which by increasing the space constant of the horizontal cell array would predict the opposite of Lankheet's et al. (1990) results. This suggests that some other mechanism is responsible for the variation in HA receptive-field size, e.g. that gap junctions coupling horizontal cells might be modulated in some way inversely with light intensity, possibly by dopamine (Hampson et al., 1992). Such an hypothesis is consistent with current theoretical analyses suggesting that an expansion of receptive-field surround is optimal at low background intensity where the problem of noise from photon fluctuation is worse (Atick & Redlich, 1992; van Hateren, 1993; Srinivasan et al., 1982).

Function of the receptive-field center

The receptive-field center of the cone is the result of several factors, the most important being optical blur and electrical coupling between cones but also including feedback from horizontal cells (Figs. 9 and 14). Although these factors produce a smooth center profile that approximates a Gaussian (Fig. 9), they serve different functions. In cat *area centralis*, the optical blur function is wider (22 μm diameter, Robson & Enroth-Cugell, 1978) than cone spacing (6 μm at 1-deg eccentricity, Smith & Sterling, 1990), so it reduces aliasing in the cone array (Levitan & Buchsbaum, 1993). Electrical coupling between cones, since it operates on the image already sampled by the cone outer segment, cannot reduce aliasing noise that (if not for optical blur) might appear in cone sampling, but can reduce aliasing noise from sampling in the next array (bipolar cells).

If aliasing were the only problem, the simplest solution would be to blur the image optically down to the spatial-frequency cutoff of higher-order neurons such as the beta ganglion cell. Yet it is apparent that optical blur is held to just over the minimum needed to prevent aliasing in the cone array. This permits additional blur required by the bipolar cell array to be accomplished by electrical coupling between cones (Levitan & Buchsbaum, 1993). The advantage is that electrical coupling also reduces noise (Lamb & Simon, 1976) that originates in Poisson photon fluctuation, channel fluctuation, and the biochemical cascade in the outer segment (Banks et al., 1987; Schnapf et al., 1990).

A cone receives signals from its neighbors through two pathways: non-inverting (gap junctions) and inverting (from horizontal cells). The spatial extent of the two signals overlaps to a large extent so it might appear that over this extent they cancel each other (see Figs. 8 and 10), which would imply a compromise in function between center and surround. Such a compromise is resolved by the observation that feedback from the horizontal cell is indirect and slow, and electrical coupling, being direct and fast, serves a different function (i.e. noise reduction) which does not directly compete with feedback. This observation is consistent with the expansion of the X ganglion cell receptive-field center at high temporal frequency (Frishman et al., 1987).

Conclusion

Our results suggest that the cone pedicle circuit generates a center-surround receptive field that performs several closely related functions. The center is shaped by optical blur and electrical coupling, and to a lesser degree by feedback. It serves at

least two functions: (1) to prevent aliasing in cone and bipolar cell, and (2) to spatially filter signal and noise in the cone pedicle. The surround, shaped by two horizontal cell types and electrical coupling, serves at least two functions: (1) to optimize signal transfer from cone outer segment to pedicle, and (2) to optimize signal transfer through the first chemical synapse.

We have presented evidence here and elsewhere (Smith & Sterling, 1990) that the beta ganglion cell receptive field arises to a large extent from the cone receptive field. It is often asked: why perform the major bandpass filtering operations at the cone, since in a linear system they could be done at any level? The answer appears to be that both center and overlapping dome-shaped surround are necessary to filter the visual signal before it passes through a noisy synapse to the second-order neural array (Laughlin et al., 1987). Yet, however critical the need for a spatial filter in the outer plexiform layer, if the filter were spatially or temporally too wide, a higher-order neuron would suffer a loss in resolution. Therefore, the dimensions and dynamic nature of the cone receptive field appear to be a delicate compromise between a local need for signal compression and the brain's requirement for spatial and temporal resolution.

Acknowledgments

I thank Peter Sterling, Noga Vardi, and Ralph Nelson for helpful discussions about this work; Paul Mueller and John Weisel for the generous sharing of computer resources that made this work possible; Norberto Grzywacz and Michael Freed for helpful criticism on the manuscript; and Sanjay Kumar and Peter Auerbach for their help with Fig. 1. This work was supported by grants MH48168, T32-EY-07035, and EY00828.

References

ATICK, J.J. & REDLICH, A.N. (1992). What does the retina know about natural scenes? *Neural Computation* **4**, 196–210.

ATTWELL, D., WERBLIN, F.S., WILSON, M. & WU, S. (1983). A sign-reversing pathway from rods to double and single cones in the retina of the tiger salamander. *Journal of Physiology* **336**, 313–333.

ATTWELL, D., WILSON, M. & WU, S.M. (1984). A quantitative analysis of interactions between photoreceptors in the salamander (*Ambystoma*) retina. *Journal of Physiology* **352**, 703–737.

ATTWELL, D. (1986). Ion channels and signal processing in the outer retina. *Quarterly Journal of Experimental Physiology* **71**, 497–536.

ATTWELL, D., MOBBS, P., TESSIER-LAVIGNE, M. & WILSON, M. (1987). Neurotransmitter-induced currents in retinal bipolar cells of the axolotl, *Ambystoma mexicanum*. *Journal of Physiology* **387**, 125–161.

BANKS, M.S., GEISLER, W.S. & BENNETT, P.J. (1987). The physical limits of grating visibility. *Vision Research* **27**, 1915–1924.

BAYLOR, D.A., FUORTES, M.G.F. & O'BRYAN, P.M. (1971). The receptive fields of cones in the retina of the turtle. *Journal of Physiology* **214**, 265–294.

BELGUM, J.H. & COPENHAGEN, D.R. (1988). Synaptic transfer of rod signals to horizontal and bipolar cells in the retina of the toad (*Bufo Marinus*). *Journal of Physiology* **396**, 225–245.

BLOOMFIELD, S.A. & MILLER, R.F. (1982). A physiological and morphological study of the horizontal cell types of the rabbit retina. *Journal of Comparative Neurology* **208**, 288–303.

BOYCOTT, B.B., PEICHL, L. & WÄSSLE, H. (1978). Morphological types of horizontal cell in the retina of the domestic cat. *Proceedings of the Royal Society B* (London) **203**, 229–245.

BURKHARDT, D.W. (1993). Synaptic feedback, depolarization, and color opponency in cone photoreceptors. *Visual Neuroscience* **10**, 981–989.

CHUN, M.H. & WÄSSLE, H. (1989). GABA-like immunoreactivity in the cat retina, electron microscopy. *Journal of Comparative Neurology* **279**, 55–67.

CLELAND, B.G., HARDING, T.H. & TULUNAY-KEESEY, U. (1979). Visual resolution and receptive-field size, examination of two kinds of cat retinal ganglion cell. *Science* **205**, 1015–1017.

COHEN, E.D. & STERLING, P. (1989). Microcircuitry related to the receptive-field center of the on-beta ganglion cell. *Journal of Neurophysiology* **65**, 352–359.

COOLEY, J.W. & DODGE, F.A. (1966). Digital computer solutions for excitation and propagation of the nerve impulse. *Biophysical Journal* **6**, 583–599.

DACHEUX, R.A. & RAVIOLA, E. (1982). Horizontal cells in the retina of the rabbit. *Journal of Neuroscience* **2**, 1486–1493.

DETWILER, P.B. & HODGKIN, A.L. (1979). Electrical coupling between cones in turtle retina. *Journal of Physiology* **291**, 75–100.

FALK, G. & FATT, P. (1972). Physical changes induced by light in the rod outer segment of vertebrates. In *Handbook of Sensory Physiology, Vol. VII/1. Photochemistry of Vision*, ed. DARTNALL, H.J.A., pp. 200–244. Berlin: Springer.

FISHER, S.K. & BOYCOTT, B.B. (1974). Synaptic connections made by horizontal cells within the outer plexiform layer of the retina of the cat and the rabbit. *Proceedings of the Royal Society B* (London) **186**, 317–331.

FOERSTER, M.H., VAN DE GRIND, W.A. & GRÜSSER, O.-J. (1977). Frequency transfer properties of three different types of cat horizontal cells. *Experimental Brain Research* **29**, 347–366.

FREED, M.A. (1992). GABA-ergic circuits in mammalian retina. In *Progress in Brain Research, GABA in the Retina and in the Central Nervous System*, ed. MIZE, R.R., MARC, R.E. & SILLITO, A., pp. 107–132, Amsterdam: Elsevier.

FRISHMAN, L.J., FREEMAN, A.W., TROY, J.B., SCHWEITZER-TONG, D.E. & ENROTH-CUGELL, C.E. (1987). Spatio-temporal responses of cat retinal ganglion cells. *Journal of General Physiology* **89**, 559–628.

HAMPSON, E.C.G.M., VANEY, D.I. & WEILER, R. (1992). Regulation of gap-junction permeability between A-type horizontal cells in rabbit retina, effects of pH and dopamine. *Investigative Ophthalmology and Visual Science* **33**, 1406.

HINES, M. (1984). Efficient computation of branched nerve equations. *International Journal of Biomedical Computing* **15**, 69–76.

HSU, A. & SMITH, R.G. (1994). Simulating the foveal cone receptive field. In *Computation and Neurons and Neural Systems*, ed. EECKMAN, F.H., pp. 73–78. Boston, MA: Kluwer Academic Publishers.

HSU, A., SMITH, R.G. & STERLING, (1994). Functional architecture of Henle's layer in the fovea of *M. Fascicularis* (submitted).

HUGHES, T.E., GRUNERT, U. & KARTEN, H.J. (1991). GABA-A receptors in the retina of the cat. An immunohistochemical study of whole-mounts, sections and dissociated cells. *Visual Neuroscience* **6**, 229–238.

KOLB, H. (1970). Organization of the outer plexiform layer of the primate retina. Electron microscopy of Golgi-impregnated cells. *Philosophical Transactions of the Royal Society B* (London) **258**, 261–283.

KOLB, H. (1974). The connections between horizontal cells and photoreceptors in the retina of the cat, electron microscopy of Golgi preparations. *Journal of Comparative Neurology* **155**, 1–14.

KOLB, H. (1977). The organization of the outer plexiform layer in the retina of the cat, electron microscopic observations. *Journal of Neurocytology* **6**, 131–153.

KRAFT, T.W. & BURKHARDT, D.A. (1986). Telodendrites of cone photoreceptors, structure and probable function. *Journal of Comparative Neurology* **249**, 13–27.

LAMB, T.D. & SIMON, E.J. (1976). The relation between intercellular coupling and electrical noise in turtle photoreceptors. *Journal of Physiology* **263**, 257–286.

LANKHEET, M.J.M., FRENS, M.A. & VAN DE GRIND, W.A. (1990). Spatial properties of horizontal cell responses in the cat retina. *Vision Research* **30**, 1257–1275.

LANKHEET, M.J.M., VAN WEZEL, R.J.A. & VAN DE GRIND, W.A. (1991). Effects of background illumination on cat horizontal cell responses. *Vision Research* **31**, 919–932.

LANKHEET, M.J.M., PRZYBYSZEWSKI, A.W. & VAN DE GRIND, W.A. (1993). The lateral spread of light adaptation in cat horizontal cell responses. *Vision Research* **33**, 1173–1184.

LASANSKY, A. (1971). Synaptic organization of cone cells in the turtle retina. *Philosophical Transactions of the Royal Society B* (London) **262**, 365–381.

LASANSKY, A. (1973). Organization of the outer layer in the retina of

the larval tiger salamander. *Philosophical Transactions of the Royal Society B* (London) **265**, 471–489.

LASANSKY, A. (1981). Synaptic action mediating cone responses to annular illumination in the retina of the larval Tiger Salamander. *Journal of Physiology* (London) **310**, 205–214.

LAUGHLIN, S.B., HOWARD, J. & BLAKESLEE, B. (1987). Synaptic limitations to contrast coding in the retina of the blowfly *Calliphora*. *Proceedings of the Royal Society B* (London) **231**, 437–467.

LEVITAN, B. & BUCHSBAUM, G. (1993). Signal sampling and propagation through multiple cell layers in the retina, modeling and analysis with multirate filtering. *Journal of the Optical Society of America* **10**, 1463–1480.

MANGEL, S.C. (1991). Analysis of the horizontal cell contribution to the receptive-field surround of ganglion cells in the rabbit retina. *Journal of Physiology* **442**, 211–234.

MURAKAMI, M., SHIMODA, Y., NAKATANI, K., MIYACHI, E. & WATANABE, S. (1982). GABA-mediated negative feedback from horizontal cells to cones in carp retina. *Japanese Journal of Physiology* **32**, 911–926.

NELSON, R. (1977). Cat cones have rod input, a comparison of the response properties of cones and horizontal cell bodies in the retina of the cat. *Journal of Comparative Neurology* **172**, 109–136.

NORMANN, R.A., PERLMAN, I., KOLB, H., JONES, J. & DALY, S.J. (1984). Direct excitatory interactions between cones of different spectral types in the turtle retina. *Science* **224**, 625–627.

PEICHL, L. & GONZALEZ-SORIANO, J. (1994). Morphological types of horizontal cell in rodent retinae: A comparison of rat, mouse, gerbil, and guinea pig. *Visual Neuroscience* **11**, 501–517.

PFLUG, R., NELSON, R. & AHNHELT, P.K. (1990). Background-induced flicker enhancement in cat retinal horizontal cells. I. Temporal and spectral properties. *Journal of Neurophysiology* **64**, 313–325.

PICCOLINO, M., NEYTON, J. & GERSHENFELD, H. (1981). Center-surround antagonistic organization in small-field luminosity horizontal cells of turtle retina. *Journal of Neurophysiology* **45**, 363–375.

POURCHO, R. G., OWCZARZAK, M. T. (1989). Distribution of GABA immunoreactivity in the cat retina, a light- and electron-microscopic study. *Visual Neuroscience* **2**, 425–435.

RAVIOLA, E. & GILULA, N.B. (1975). Intramembrane organization of specialized contacts in the outer plexiform layer of the retina, a freeze-fracture study in monkeys and rabbits. *Journal of Cell Biology* **65**, 192–222.

ROBSON, J.G. & ENROTH-CUGELL, C.E. (1978). Light distribution in the cat's retinal image. *Vision Research* **18**, 159–173.

SARTHY, P.V. & FU, M. (1989). Localization of L-glutamic acid decarboxylase mRNA in cat retina horizontal cells by *in situ* hybridization. *Journal of Comparative Neurology* **288**, 593–600.

SCHNAPF, J.L., NUNN, B.J., MEISTER, M. & BAYLOR, D.A. (1990). Visual transduction in cones of the monkey, *Macaca fascicularis*. *Journal of Physiology* **427**, 681–713.

SKRZYPEK, J. & WERBLIN, F. (1983). Lateral interactions in absence of feedback to cones. *Journal of Neurophysiology* **49**, 1007–1016.

SMITH, R.G. (1992). NeuronC, a computational language for investigating functional architecture of neural circuits. *Journal of Neuroscience Methods* **43**, 83–108.

SMITH, R.G., FREED, M.A. & STERLING, P. (1986). Microcircuitry of the dark-adapted cat retina, functional architecture of the rod-cone network. *Journal of Neuroscience* **6**, 3505–3517.

SMITH, R.G. & STERLING, P. (1990). Cone receptive field in cat retina computed from microcircuitry. *Visual Neuroscience* **5**, 453–461.

SPRUSTON, N. & JOHNSTON, D. (1992). Perforated patch-clamp analysis of the passive membrane properties of three classes of hippocampal neurons. *Journal of Neurophysiology* **67**, 508–529.

SRINIVASAN, M.V., LAUGHLIN, S.B. & DUBS, A. (1982). Predictive coding, a fresh view of inhibition in the retina. *Proceedings of the Royal Society B* (London) **216**, 427–459.

STEINBERG, R.H. (1969). Rod and cone contributions to S-potentials from the cat retina. *Vision Research* **9**, 1319–1329.

SUZUKI, S., TACHIBANA, M. & KANEKO, A. (1990). Effects of glycine and GABA on isolated bipolar cells of the mouse retina. *Journal of Physiology* **421**, 645–662.

TACHIBANA, M. & KANEKO, A. (1984). Gamma-aminobutyric acid acts at axon terminals of turtle photoreceptors, difference in sensitivity among cell types. *Proceedings of the National Academy of Sciences of the U.S.A.* **81**, 283–294.

TRANCHINA, D., SNEYD, J. & CADENAS, I.D. (1991). Light adaptation in turtle cones, testing and analysis of a model for transduction. *Biophysical Journal* **60**, 217–237.

TSUKAMOTO, Y., SMITH, R.G. & STERLING, P. (1990). Collective coding improves signal-to-noise ratio in ganglion cells. *Proceedings of the National Academy of Sciences of the U.S.A.* **87**, 1860–1864.

VAN DE GRIND, W.A. & GRÜSSER, O.-J. (1981). Frequency transfer properties of cat retina horizontal cells. *Vision Research* **21**, 1565–1572.

VAN HATEREN, J.H. (1993). Spatiotemporal contrast sensitivity of early vision. *Vision Research* **33**, 257–267.

VANEY, D.I. (1991). Many diverse types of retinal neurons show tracer coupling when injected with biocytin or Neurobiotin. *Neuroscience Letters* **125**, 187–190.

VANEY, D.I. (1993). The coupling pattern of axon-bearing horizontal cells in the mammalian retina. *Proceedings of the Royal Society B* (London) **252**, 93–101.

VARDI, N., KAUFMAN, D.L. & STERLING, P. (1994). Horizontal cells in cat and monkey retina express different isoforms of glutamic acid decarboxylase. *Visual Neuroscience* **11**, 135–142.

VARDI, N. & STERLING, P. (1994). Subcellular localization of $GABA_A$ receptor on bipolar cells in macaque and human retina. *Vision Research* **34**, 1235–1246.

WÄSSLE, H. (1971). Optical quality of the cat eye. *Vision Research* **11**, 995–1006.

WÄSSLE, H., BOYCOTT, B.B. & PEICHL, L. (1978*a*). Receptor contacts of horizontal cells in the retina of the domestic cat. *Proceedings of the Royal Society B* (London) **203**, 247–267.

WÄSSLE, H., PEICHL, L. & BOYCOTT, B.B. (1978*b*). Topography of horizontal cells in the retina of the domestic cat. *Proceedings of the Royal Society B* (London) **203**, 269–291.

WERBLIN, F.S. (1971). Adaptation in a vertebrate retina: Intracellular recording in Necturus. *Journal of Neurophysiology* **34**, 228–241.

WERBLIN, F.S. (1974). Control of retinal sensitivity, II Lateral interactions at the outer plexiform layer. *Journal of General Physiology* **63**, 62–87.

WU, S.M. (1991). Input-output relations of the feedback synapse between horizontal cells and cones in the tiger salamander retina. *Journal of Neurophysiology* **65**, 1197–1206.

YEH, H.H., LEE, M.B. & CHEUN, J.E. (1990). Properties of GABA-activated whole-cell currents in bipolar cells of the rat retina. *Visual Neuroscience* **4**, 349–357.

Appendix

Derivation of optimal impedance match for cone

Simplifying a cone into two conductances, *Ros* (the outer segment resistance) and *Rp* (the pedicle leakage resistance), and one battery, *Vos* (the outer segment driving potential), the cone's resting voltage is

$$Vp = Vos * Rp/(Rp + Ros) \tag{1}$$

A low-contrast light flash reduces the outer segment conductance by a small amount to a new value, *Rosf*. The voltage response at the pedicle is *Vpf*:

$$Vpf = Vos * Rp/(Rp + Rosf) \tag{2}$$

The light response at the pedicle is the difference between the flash response and the steady-state response:

$$Vpf - Vp = Vos * Rp * [1/(Rp + Rosf) - 1/(Rp + Ros)] \tag{3}$$

Assuming that *Ros* is nearly equal to *Rosf*, the derivative of this function with respect to *Rp* simplifies to

$$d(Vpf - Vp)/d(Rp) = Vos * (Ros - Rosf) * [1/(Rp + Ros)^2 - 2 * Rp/(Rp + Ros)^3] \quad (4)$$

Setting this derivative to zero, Rp equals Ros.

This result implies that the maximum transfer of a low-contrast signal to the pedicle occurs when the membrane resistance of axon and pedicle is equal to the outer segment membrane resistance. Although in reality cones are more complex than this, a more realistic derivation that includes factors for axial and membrane resistance of the cone axon gives a similar conclusion (Hsu et al., 1994).